

Bulk and Emulsion Copolymerizations of *n*-Butyl Acrylate and Poly(methyl methacrylate) Macromonomer

P. RAJATAPITI,^{1,2} V. L. DIMONIE,¹ and M. S. EL-AASSER^{1,3,*}

Emulsion Polymers Institute¹ and Departments of Materials Science and Engineering² and Chemical Engineering³, Lehigh University, Bethlehem, Pennsylvania 18015

SYNOPSIS

Bulk and emulsion copolymerizations of an ω -unsaturated poly(methyl methacrylate) (PMMA) macromonomer with *n*-butyl acrylate (*n*-BA) were investigated. The reactivity of PMMA macromonomer in bulk copolymerization with *n*-BA was found to be lower than that of methyl methacrylate monomer with *n*-BA. The incorporation of PMMA macromonomer into poly(butyl acrylate) (PBA) latex particles by miniemulsion copolymerization was proved by high performance liquid chromatography–silica adsorption spectroscopy. Dynamic mechanical studies showed that PMMA macromonomer was grafted to the PBA backbone, and the degree of grafting increased as the ratio of PMMA macromonomer to *n*-BA increased. Microphase separation of the PMMA macromonomer grafts was observed at higher ratio of macromonomer (higher or equal to 10% weight of macromonomer based on total polymer phase). The *n*-BA/PMMA macromonomer copolymer behaved completely differently from the physical blend of PBA and PMMA macromonomer particles of the same composition. © 1996 John Wiley & Sons, Inc.

INTRODUCTION

Block or graft copolymers can be used as compatibilizing agents to improve the interfacial characteristics between the different polymer phases. However, graft copolymers are less widely used as compatibilizing agents than block copolymers because the molecular structures of these graft copolymers, which are commonly prepared by chemical grafting reactions, are difficult to characterize and the experimental techniques for controlling these grafting reactions are limited as well.^{1–2} Since Milkovich and Chiang developed the method of preparing copolymers with uniform grafts using the macromonomer technique, the synthesis of macromonomers and the copolymerization of macromonomers and comonomers have been studied extensively.^{3–6} Nevertheless, little has been published on the emulsion copolymerization of a water-insoluble macromonomer and a comonomer. Several authors have suggested that

the macromonomer/comonomer emulsion copolymerization occurs only when the reaction locus is in the monomer droplet.^{7–9}

The ability of the macromonomer to become involved in a copolymerization process is controlled by the reactivity ratio of the macromonomer and the comonomer. Because the physical properties of the graft copolymers are dependent on the distribution of the grafts along the backbone, the copolymerization behavior must be well understood. Regarding the copolymerization reactivity of a macromonomer, the following must be considered as major influencing factors¹⁰: (1) copolymerization reactivity of the polymerizable end group, (2) enhanced diffusion control effect associated with the large size of the macromonomer (this might lower the relative copolymerization propagation rate of the macromonomer to the comonomer, as the higher molecular weight of the macromonomer may reduce its translational diffusivity and increase the topological resistance against the segmental diffusion of the reactive end group), and (3) nonhomogeneous distribution of the polymerizable end group in the reaction media associated with the thermodynamic repulsive

* To whom correspondence should be addressed.

interaction between the macromonomer and the propagating copolymer chain and/or the incompatibility between the unlike polymers. In our studies, the reactivity ratio of *n*-butyl acrylate (*n*-BA) and poly(methyl methacrylate) (PMMA) macromonomer in bulk copolymerization was determined using the integrated form of the copolymerization equation developed by Jaacks.¹¹

Miniemulsion copolymerization was used to incorporate the PMMA macromonomer into poly-(butyl acrylate) (PBA) chains.¹² Based on the difference in the hydrophilicity between PMMA macromonomer and *n*-BA monomer, the *n*-BA/PMMA macromonomer copolymers are expected to reside at the interface of the PBA particles. These copolymers can be used as compatibilizing agents to improve the coverage of the core PBA particles by a PMMA shell in composite latex particles, when the PBA particles are used as seed in a second-stage emulsion polymerization of methyl methacrylate (MMA) monomer. The incorporation of the macromonomer was followed by high-performance liquid chromatography (HPLC)-silica adsorption spectroscopy. The dynamic mechanical properties of PBA incorporating PMMA macromonomer latex films were studied and related to the compatibility between the PBA and the PMMA phases.

EXPERIMENTAL

Materials

n-BA monomer (Aldrich) was washed with 10% aqueous sodium hydroxide solution and then with distilled-deionized water, was dried overnight (at -4°C) with anhydrous sodium sulfate (100 g/L), and finally was passed through a column packed with the inhibitor remover (Aldrich). The monomer was stored at -4°C prior to use. For the bulk copolymerization reactions, *n*-BA monomer was freshly distilled under reduced pressure at 15 mmHg before use. The PMMA macromonomer ($M_w = 5.3 \times 10^3$ g/mol, $M_w/M_n = 1.89$; du Pont) (Fig. 1) was used as received. (This macromonomer was prepared by free radical polymerization of MMA using a cobalt [II] complex [such as cobalt porphyrins or cobalttoximes] as a catalytic chain transfer agent¹³⁻¹⁵). Polystyrene ($M_w 2.9 \times 10^6$ g/mol, $M_w/M_n = 1.09$; Polymer Laboratories), azo-(bisobutyronitrile) (AIBN) (Kodak), sodium lauryl sulfate (Henkel), hexadecane (Aldrich), potassium persulfate (Fisher), tetrahydrofuran (Aldrich), 2-butanone (Aldrich), and tol-

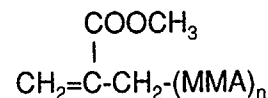


Figure 1 Structure of PMMA macromonomer. $M_w = 5.3 \times 10^3$ g/mol, $M_w/M_n = 1.89$.

uene (Aldrich) were also used with no further purifications.

Characterization and Testing

Copolymerization Reactivity Ratio: Theoretical Considerations

When two monomers, M_1 and M_2 , are copolymerized using a radical initiator, the consumption of M_1 and M_2 during the time interval ($t, t + dt$), which determines the instantaneous composition of the copolymer formed, is given by the well-known copolymer composition equation:

$$\frac{d[M_1]}{d[M_2]} = \frac{[M_1] (r_1[M_1] + [M_2])}{[M_2] (r_2[M_2] + [M_1])} \quad (1)$$

where $d[M_1]$ and $d[M_2]$ are the concentrations of M_1 and M_2 in the resulting copolymer, $[M_1]$ and $[M_2]$ are the concentrations of monomers 1 and 2 in the monomer feed, and r_1 and r_2 are their reactivity ratios. Each r_i depicts the ratio of the rate constant for a reactive propagating species adding to its own type of monomer over the rate constant for its addition to the other monomer.

In 1972 Jaacks proposed a novel method for the determination of reactivity ratios in binary and ternary copolymerizations.¹¹ He simplified the determination of reactivity ratios by using an excess of one monomer (M_1) so that the copolymer has a very small content of the other monomer (M_2). Under these circumstances, chain propagation takes place almost exclusively by addition to polymer radicals with a terminal M_1 unit. Since $[M_1] \gg [M_2]$, the following can be assumed:

$$r_1[M_1] + [M_2] = r_1[M_1] \quad (2)$$

$$r_2[M_2] + [M_1] = [M_1] \quad (3)$$

Equation 1 then reduces to

$$\frac{d[M_1]}{d[M_2]} = r_1 \frac{[M_1]}{[M_2]} \quad (4)$$

This situation is almost always encountered where M_2 is a macromonomer, because in a regular system the molar composition of the macromonomer in the feed is extremely low even at high feed ratios by weight. Therefore, the copolymerization of monomer M_1 with macromonomer M_2 can be described only by the r_1 value and monomer feed composition $[M_1]/[M_2]$. Taking the induction periods into account, the relative reactivity ratio r_1 can be estimated from the rearrangement of eq. (4):

$$\log \frac{[M_1]_t}{[M_1]_0} \approx r_1 \log \frac{[M_2]_t}{[M_2]_0} + \text{constant} \quad (5)$$

This reduced copolymerization equation became the classic method used to study the reactivity of macromonomers.^{10,17-21} The relative copolymerization reactivity of the macromonomer is normally evaluated by $1/r_1$ (i.e., k_{12}/k_{11} , the ratio of the rate constant for a propagating copolymer radical adding macromonomer to the rate constant for adding its own comonomer), because the low molar concentration of the macromonomer makes it difficult to determine the exact value of r_2 directly. Since the value of r_1 is inversely proportional to the macromonomer reactivity, the higher the value of r_1 , the less reactive is the macromonomer.

Bulk Copolymerization of *n*-BA and PMMA Macromonomer

Copolymer samples were prepared by bulk polymerization of *n*-BA and PMMA macromonomer. AIBN was used as a radical initiator. *n*-BA and PMMA macromonomer were weighed in a glass tube and AIBN was added after the macromonomer was completely dissolved. The copolymerization experiments were carried out in a water bath at 70°C under constant agitation. After a specified reaction time, the mixture was quenched with ice to stop the reaction. The degree of *n*-BA conversion was under 15% for all the macromonomer/*n*-BA ratios.

The monomer conversion was followed by gravimetry. The macromonomer conversion was followed by gel permeation chromatography (GPC; Waters Associate). The measurements were made using a differential refractometer detector, and a set of ultrastrogel columns of 10^3 , 10^4 , and 10^6 Å, operated at room temperature. Tetrahydrofuran (THF) solvent was used at a flow rate of 1 ml/min. The GPC samples were prepared by drying the copolymer samples in a vacuum oven until no traces of *n*-BA were left. The polymer was then dissolved

in THF and mixed with a THF solution of high-molecular-weight polystyrene (PS) used as an external standard. Only the peaks of the unreacted macromonomer and PS were detected from the GPC spectra. We anticipate that the copolymer may become highly branched and/or crosslinked upon drying, as evidenced by the high viscosity of the solution. This branched and/or crosslinked copolymer was then filtered out before the sample was injected into the GPC. It is not clear how the chains become branched and/or crosslinked; however, this phenomenon is possibly related to the presence of the residual cobalt from the PMMA macromonomer synthesis. (It is well known that cobalt salts are widely used as efficient autoxidant catalysts in paint formulations²²). Conversions of the macromonomer at given copolymer feed ratios were determined from the relative peak area of a high-molecular-weight PS standard to that of an unreacted macromonomer using a calibration curve, which was developed by injecting samples of known weights of PS standard and PMMA macromonomer into the GPC. The area ratios of PS and PMMA macromonomer peaks in these samples were then determined from the chromatograms. An example of a typical GPC chromatogram of the PS standard-PMMA macromonomer mixture in THF is shown in Figure 2. At least two injections were made for each copolymer and standard solution, and the results were averaged. A linear dependence between the weight ratio and area ratio of the polystyrene standard and PMMA macromonomer was obtained, as shown in Figure 3.

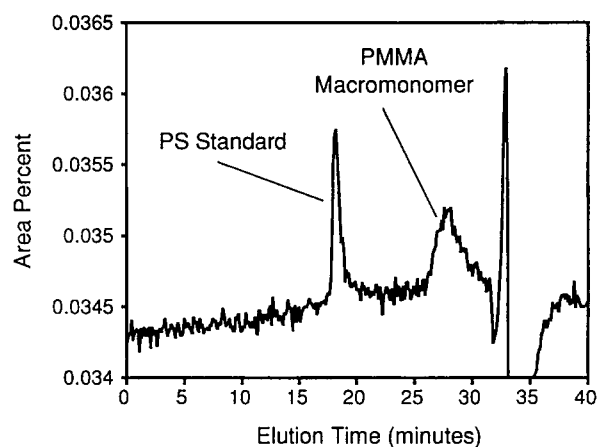


Figure 2 A GPC chromatogram of a mixture of PS standard ($M_w 2.9 \times 10^6$ g/mol, $M_w/M_n = 1.09$) and PMMA macromonomer ($M_w = 5.3 \times 10^3$ g/mol, $M_w/M_n = 1.89$) in THF.

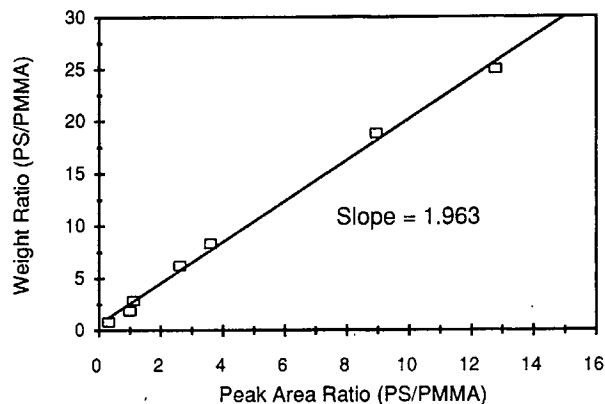


Figure 3 The relationship weight ratio versus GPC peak area ratio of a high molecular weight PS standard and PMMA macromonomer.

HPLC–Silica Adsorption Chromatography

Graft copolymers of *n*-BA and PMMA macromonomer were characterized using HPLC–silica adsorption chromatography with a solvent gradient. The copolymers were synthesized by miniemulsion copolymerization. The copolymerization procedure has been described in detail elsewhere.¹² The copolymer solutions in toluene were prepared by azeotropic distillation of the latexes. In this method, toluene was added to the latex to form an azeotropic mixture with water present in the latex serum and distilled using a vacuum evaporator (Flash Evaporator, Buchler Instruments) until all the water was removed. Polymer samples were eluted using a toluene/2-butanone mixture with a gradient changing from 98% : 2% toluene/2-butanone to 100% 2-butanone in 30 min. Evaporative light scattering was the detection method.

Differential Scanning Calorimetry

The glass transition temperature (T_g) of the macromonomer was determined using differential scanning calorimetry (DSC) (Mettler DSC Model-30). The sample was weighed (0.15–0.30 mg) in an aluminum pan and placed in the heating chamber of the differential scanning calorimeter. The measurements were run in the temperature range of -50°C to 120°C . The heating rate was $10^\circ\text{C}/\text{min}$. The sample was analyzed twice; the first run was performed to eliminate any thermal history while the second run measured the T_g .

Dynamic Mechanical Studies

Samples were prepared by air-drying the PBA latexes on folded release paper and cutting the films

to the desired shape. The sample dimensions were on the order of $1 \times 10 \times 25$ mm. Experiments were performed on the Rheometric Solids Analyzer (RSA II), which applies a tensile strain to the sample, using thin-film geometry. The films were analyzed in the temperature-sweep mode in a dry nitrogen atmosphere at the frequency of 6.28 rad/s and over a temperature range of -100°C to 200°C . Data were recorded every 5°C .

RESULTS AND DISCUSSION

Reactivity Ratio of *n*-BA and PMMA Macromonomer in Copolymerization

Graft copolymers possess physical properties that are dependent not only on their compositions but also on their uniformity of macromonomer incorporation. The PMMA macromonomer used in our project has been demonstrated to not undergo homopolymerization either by solution (in benzene, 60°C , AIBN)²¹ or by miniemulsion.⁹ Cacioli and colleagues²¹ also studied the copolymerization of this macromonomer ($M_n = 1 \times 10^3$ g/mol) with ethyl acrylate (EA) (in benzene, 60°C , AIBN). They reported that the copolymer, taken at high conversion, gave a composition very nearly identical to that of the feed.²¹ In this paper we describe our attempt to access the homogeneity of the product composition by determining the reactivity ratio of the macromonomer with the comonomer.

Figure 4 presents the plot of $-\log([M_2]_t/[M_2]_0)$ versus $-\log([M_1]_t/[M_1]_0)$ for the *n*-BA/PMMA

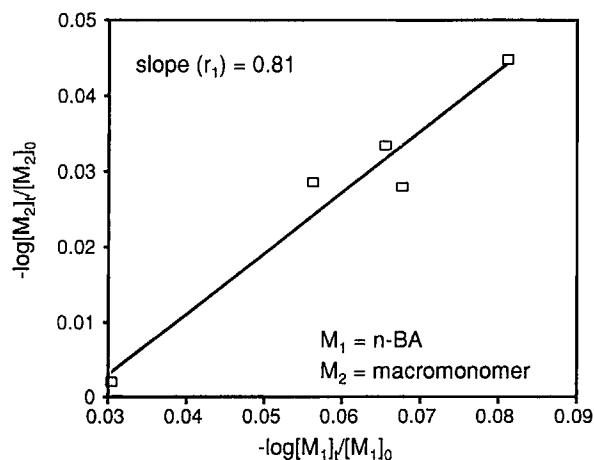


Figure 4 $-\log([M_2]_t/[M_2]_0)$ vs. $-\log([M_1]_t/[M_1]_0)$ for the *n*-BA/PMMA macromonomer pair; $M_1 = n$ -BA and $M_2 =$ PMMA macromonomer.

Table I Free Radical Copolymerization Reactivity Ratios

Monomer ₁ /Monomer ₂	r_1	r_2^*
<i>n</i> -BA/PMMA macromonomer (M_n macromonomer = 2.8×10^3 g/mol)	0.81	1.23
<i>n</i> -BA/MMA monomer ²⁴	0.43	1.88
	0.11	2.86
EA/PMMA macromonomer ²² (M_n macromonomer = 1.0×10^3 g/mol)	0.60	1.67
EA/MMA monomer ²⁵	0.22	2.04
	0.28	2.00
	0.47	1.83

* r_2 for PMMA macromonomer estimated from $1/r_1$.

macromonomer pair. r_1 (*n*-BA), calculated from the slope of the plot, is determined to be 0.81. As stated in the previous section, the low molar concentration of the macromonomer prevents us from directly determining the reactivity of the macromonomer (r_2). The macromonomer reactivity is then estimated by $1/r_1$, which provides information about the rate of addition of the macromonomer to the *n*-BA radical. Thus, the reactivity of the PMMA macromonomer (r_2) is approximated to equal $1/r_1 = 1.23$. Harrison studied the copolymerization of EA with PMMA macromonomer (M_n macromonomer = 1×10^3 g/mol, in benzene, 60°C, AIBN) and reported estimated reactivity ratio $r_1 = 0.6$ (and thus $r_2 \approx 1/r_1 = 1.67$).²³ Table I compares the reactivity ratios of *n*-BA/PMMA macromonomer, *n*-BA/MMA monomer,²⁴ EA/PMMA macromonomer,²³ and EA/MMA monomer.²⁵ The reactivity of PMMA macromonomer is lower than that of MMA monomer in copolymerization with either *n*-BA or EA. This reduction in reactivity of the macromonomer may be explained as resulting from excluded kinetic volume effect,^{18,20-21} steric barrier provided by the long macromonomer chain during the growing radical macromonomer reaction,^{18,21,23} or the onset of microphase separation.^{17,19}

Degree of Macromonomer Incorporation

Adsorption chromatography is an excellent technique used to measure a number of characteristic parameters for block copolymers. Nevertheless, it suffers from problems, such as quantitative detection without a chromophore, a limited number of suitable solvents, and the need for solvent gradients in the separation. These limitations show up in polymer chromatography to a greater extent than for the

more common small-molecule chromatography. Mourey has described an adsorption chromatography technique using an evaporative light-scattering detector which overcomes many of the problems listed above.²⁶ Using his technique, polymers were fractionated based on composition with very little molecular-weight dependence. In 1991, Neff and Spinelli successfully used Mourey's technique to characterize MMA and butyl methacrylate block copolymers.²⁷ These block copolymers are subject to all of the above experimental difficulties because they have no useful chromophore, and the types of solvents required for the separation of these systems are not readily used in normal detection systems.

In our work, we used HPLC-silica adsorption chromatography to determine the degree of macromonomer incorporation in the PBA seed latexes. PBA homopolymer, PMMA macromonomer, and PBA latex prepared in the presence of 10% weight macromonomer based on total polymer phase, as well as the latter sample blended with different amounts of pure PMMA macromonomer, were separated by gradient solvent elution through the same silica column under the same conditions. As suggested by the chromatograms in Figure 5, any un-polymerized macromonomer can be observed as a separate peak (after approximately 19 min elution time). For the PBA sample copolymerized with PMMA macromonomer [Fig. 5(B)], from the decrease in the area under the PBA peak and the ap-

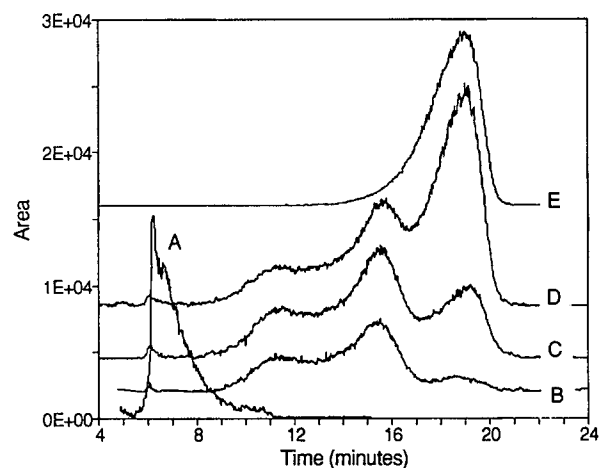


Figure 5 HPLC chromatograms of (A) PBA homopolymer; (B) PBA copolymerized with 10% by weight of macromonomer based on total polymer phase (M1053); (C) M1053 mixed with pure macromonomer (2% weight based on polymer weight); (D) M1053 mixed with pure macromonomer (10% weight based on polymer weight); and (E) PMMA macromonomer.

pearance of new shifted peaks, we concluded that most of the PBA chains were grafted with PMMA macromonomer to various degrees; some unreacted macromonomer, however, can still be observed. Based on a calibration obtained from the area under the PMMA macromonomer peak in copolymer sample (B), and in samples C and D, in which copolymer sample (B) was blended with known amounts of pure PMMA macromonomer, it was estimated that over 90% of the PMMA macromonomer was converted to the PBA/PMMA macromonomer graft copolymer in copolymer sample (B).

Dynamic Mechanical Studies of PBA Latexes

The dynamic mechanical spectroscopy (DMS) experiment typically involves the application of small-amplitude oscillatory strains to the polymer sample, and the measurement of the resulting sinusoidal stress response. The mechanical energy given to the sample is either stored elastically or is dissipated through the increased molecular motion. The tensile storage modulus (E') represents the ability of a material to store energy elastically, whereas the tensile loss modulus (E'') indicates the sample's ability to dissipate energy. $\tan \delta$, which is the ratio of E''/E' , is the tangent of the phase angle shift between the strain and the resultant stress of the sample. It can also be used as a measure of the sample's damping properties.

The DMS technique has been widely used to investigate the relationship between the filler and the matrix in block and graft copolymers. The temperature dependence of the dynamic modulus reflects the extent of phase separation of the filler and the matrix. Generally, block or graft copolymers which show a complete phase mixing (i.e., the two segments are compatible) have one single transition in between those of the corresponding homopolymers. When the two segments are incompatible and phase separation occurs, the copolymer has two transitions identical to that of the corresponding homopolymers. With a partial phase mixing and/or a diffuse interface, the transition obtained would be different from that of either constituent homopolymer. The slope of the curve through the transition would become less steep, which indicates a more gradual decrease in modulus over a wider temperature range. In our studies, the degree of compatibility between the PBA and PMMA chains in the latex particles was determined by the analysis of the dried polymer latex films. The DMS measurement results were compared between films made from PBA latexes

prepared in the absence and the presence of the PMMA macromonomer, at different weight ratios of the PMMA macromonomer to the total polymer phase. The results are shown in Figures 6–8.

The DMS data showed that for the PBA latexes copolymerized with PMMA macromonomer, both the E' and E'' values in the rubbery plateau region (approximately between -40°C and 90°C) are higher than the values for the PBA homopolymer. Both E' and E'' values also increase with PMMA macromonomer content. These data are consistent with a reinforcing of the soft PBA polymer by the glassy PMMA polymer. In addition to the incorporation of the more rigid PMMA grafts into the soft PBA backbone, during the film-forming process the relatively low-molecular-weight PMMA graft segments may aggregate into discrete domains of a few hundred Å. This phenomenon can be explained by the flexibility of the PBA backbone, which allows the PMMA macromonomer segments to aggregate and to form PMMA macromonomer domains. These domains, dispersed in a continuous backbone PBA matrix, further act as fillers and physical crosslinking sites in the soft PBA phase.

The length of the rubbery plateau region can generally be related to the molecular weight of the rubbery polymer chains.²⁸ When *n*-BA was copolymerized with PMMA macromonomer, the segment length of the PBA blocks became shorter than the length of the PBA homopolymer chain. The higher the ratio of PMMA macromonomer to the total polymer phase, the shorter the length of each PBA

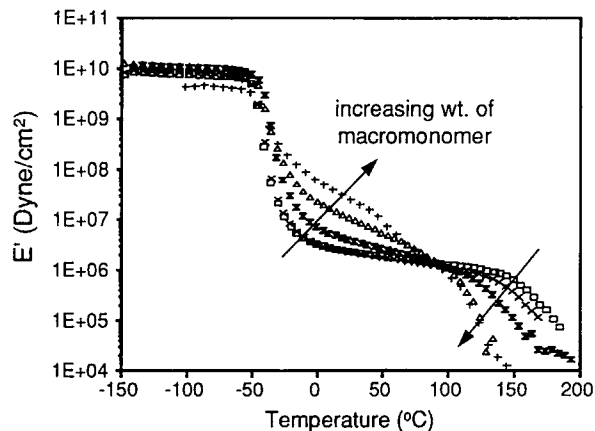


Figure 6 Temperature dependence of the tensile storage modulus (E') for PBA homopolymer and PBA incorporating different wt % of PMMA macromonomer based on total polymer phase. (\square) PBA homopolymer, and PBA incorporating (\times) 2, (\otimes) 5, (\triangle) 10, and ($+$) 20% weight PMMA macromonomer based on total polymer phase.

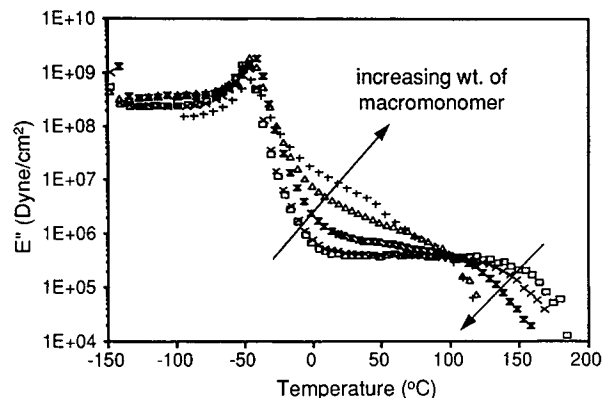


Figure 7 Temperature dependence of the tensile loss modulus (E'') for PBA homopolymer and PBA incorporating different wt % of PMMA macromonomer based on total polymer phase. (\square) PBA homopolymer, and PBA incorporating (\times) 2, (X) 5, (Δ) 10, and ($+$) 20% weight PMMA macromonomer based on total polymer phase.

segment. This is reflected in the long rubbery plateau regions for both the E' and the E'' spectra of the PBA homopolymer. For PBA incorporating PMMA macromonomer, the plateau regions are shorter and the length of the plateaus decreases with the increasing ratio of PMMA macromonomer to the total polymer phase. In the samples where the weight of the PMMA macromonomer was higher than or equal to 10% based on the total polymer phase, a transition was also observed at approximately 100°C. This would correspond to the T_g for the PMMA macromonomer domains formed from the PMMA grafts of the copolymer. (The T_g of the PMMA macromonomer, which was measured by DSC at the minimum in the peak of the derivative heat flow curve, was found to be approximately 101°C, in good agreement with the value reported for PMMA, 105°C²⁹). At lower macromonomer contents, the number of the macromonomer grafts may not be high enough to form separate PMMA domains and thus this transition could not be observed. $\tan \delta$ peak maxima of the rubbery phase (between -50°C and -10°C) broadened with increasing PMMA macromonomer content. This broadening of the peaks suggests the large distribution in composition of the graft copolymers. The height of the $\tan \delta$ peaks can be related to the volume fraction of ungrafted PBA in the polymer. These results show that more PBA was grafted to the PMMA macromonomer as the ratio of PMMA macromonomer to *n*-BA increased. Moreover, a shift in the $\tan \delta$ peaks toward higher temperatures was observed as the weight ratio of PMMA macromonomer was increased from 0%

to 2% and 5% weight based on the total polymer phase (-37.5, -36, and -32°C, respectively). This also suggests an incorporation of PMMA into PBA chains and a better miscibility with the PBA homopolymer chains. At the higher weight ratios of 10% and 20%, the peaks shift back to -37°C and -40°C, respectively. This could be the result of phase separation as the PMMA grafts of the copolymer form larger domains. The values of the $\tan \delta$ maxima were higher than the T_g reported for PBA in literature (-46°C³⁰). This may be due to the difference in the glass transition definition. The $\tan \delta$ maximum represents the midpoint T_g , whereas the E'' maximum represents the starting point of the transition. Therefore the $\tan \delta$ maximum always appears several degrees higher than the E'' maximum. A small but noticeable peak at approximately 100°C was also observed for the latter two samples (prepared at higher PMMA macromonomer contents). This supports the earlier conclusion that when the ratio of PMMA macromonomer to the total polymer phase is higher than or equal to 10%, PMMA macromonomer grafts from the copolymer form phase-separated domains large enough for an independent T_g of PMMA macromonomer to be detected.

For comparison, a blend of PBA and PMMA macromonomer was subjected to the same testing procedure. The blend was prepared from a PBA latex and a PMMA macromonomer artificial latex. The

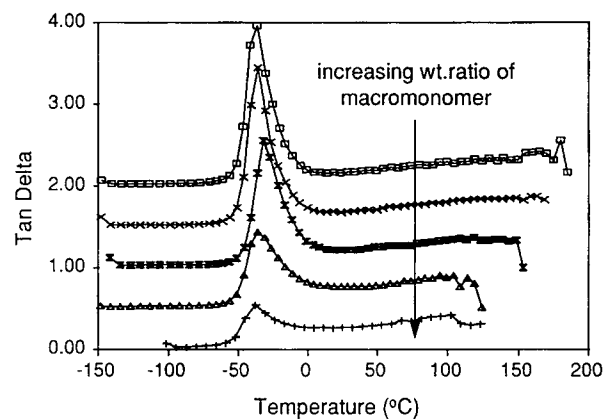


Figure 8 A stack plot of temperature dependence of the $\tan \delta$ for PBA homopolymer and PBA incorporating different wt % of PMMA macromonomer based on total polymer phase. (\square) PBA homopolymer, and PBA incorporating (\times) 2, (X) 5, (Δ) 10, and ($+$) 20% weight PMMA macromonomer based on total polymer phase. Measurement values were shifted along the y-axis by 2.0, 1.5, 1.0, 0.5, and 0, respectively.

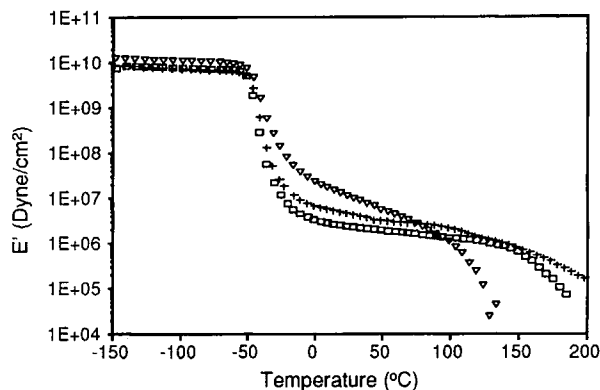


Figure 9 Temperature dependence of the tensile storage modulus (E') of PBA homopolymer (□), PBA blended with macromonomer (+), and PBA incorporating PMMA macromonomer (▽); 10% weight of macromonomer based on total polymer phase.

PMMA macromonomer latex was prepared using the same recipe as that for the preparation of the PBA seed latex, with the difference that toluene was used instead of the *n*-BA monomer (10% weight PMMA macromonomer based on the total oil phase). Toluene was then removed by vacuum stripping at 45°C (Flash Evaporator, Buchler Instruments) to create an artificial latex of PMMA macromonomer in water. Figures 9–11 show a comparison of the E' , the E'' , and the $\tan \delta$ spectra of pure PBA latex, PBA copolymerized with PMMA macromonomer, and PBA blended with PMMA macromonomer particles (10% weight macromonomer based on total polymer phase).

When PMMA macromonomer was blended directly with the PBA seed latexes, the DMS response of the dried films is very similar to the PBA itself, and much different from the PBA latex copolymerized with PMMA macromonomer. The E' and E'' values in the rubbery plateau region (between -40°C and 150°C) of the blend are only slightly higher than those of the PBA homopolymer. The PBA chains in the PBA homopolymer and the blend are relatively the same length and thus both showed long rubbery plateau regions. Although a small peak in the $\tan \delta$ curve was detected at approximately 100°C for both the blend and the copolymer sample, the height of the $\tan \delta$ peak of the rubbery phase in the blend was only slightly altered when the PBA latex was blended with the PMMA macromonomer particles. This agrees with the earlier conclusion that the PMMA macromonomer was chemically incorporated into the PBA chains of the copolymer sample. Figure 12 shows a schematic of the films cast

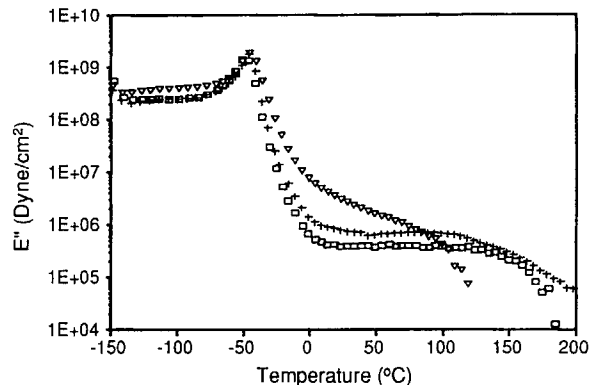


Figure 10 Temperature dependence of the tensile loss modulus (E'') for PBA homopolymer (□), PBA blended with macromonomer (+), and PBA incorporating PMMA macromonomer (▽); 10% weight of macromonomer based on total polymer phase.

from (A) PBA particles prepared in the presence of PMMA macromonomer and from (B) PBA particles blended with PMMA macromonomer particles. This figure is based on our earlier conclusion that when macromonomer was copolymerized with *n*-BA, the graft copolymer formed was preferentially partitioned on the surface of the particle.¹² During the film-forming process, the low-molecular-weight PMMA macromonomer segments will aggregate into discrete domains at the particle's interface, acting similar to a distinct PMMA phase. On the other hand, when the macromonomer particles are directly blended with PBA particles in the latex form the PMMA stays as small domains evenly dispersed

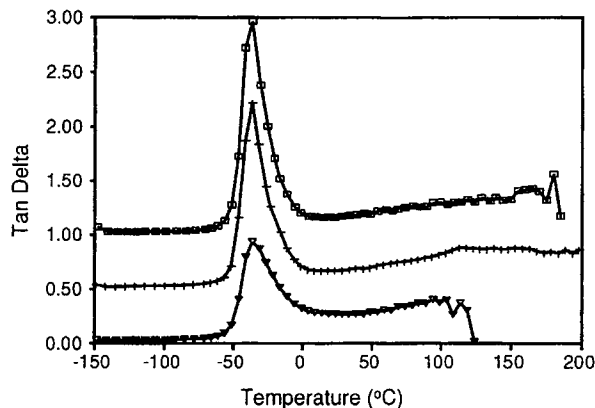


Figure 11 A stack plot of temperature dependence of the $\tan \delta$ for for PBA homopolymer (□), PBA blended with macromonomer (+), and PBA incorporating PMMA macromonomer (▽); 10% weight of macromonomer based on total polymer phase. Measurement values were shifted along the y-axis by 1.0, 0.5, and 0, respectively.

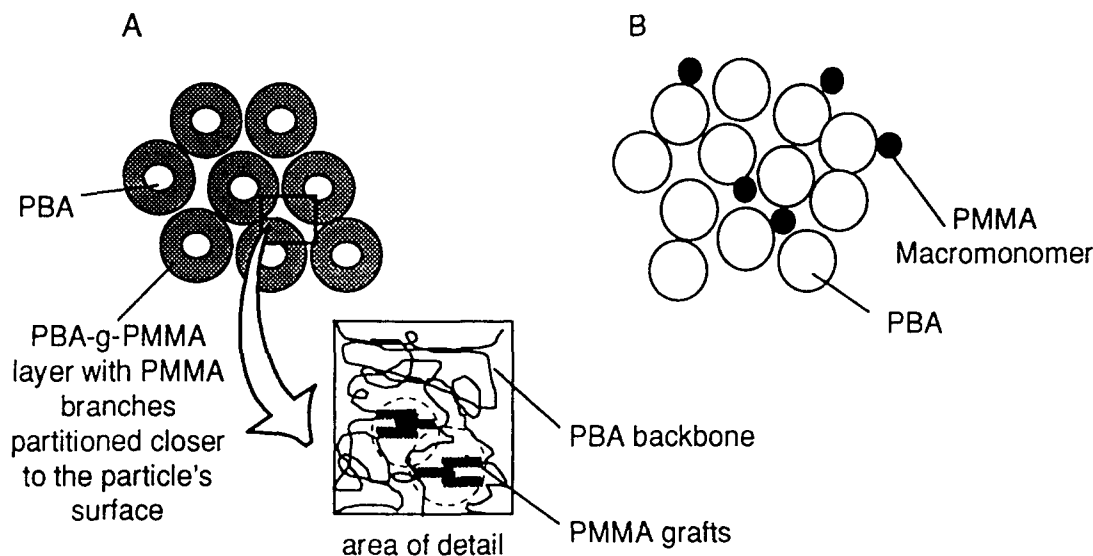


Figure 12 Schematic of the films cast from (A) PBA incorporating PMMA macromonomer particles, and (B) PBA particles blended with PMMA macromonomer particles.

within the PBA continuous phase when directly blended with PBA in the latex form. The size of these domains is too small to act as PMMA fillers reinforcing the PBA matrix and to modify the PBA film properties.

CONCLUSIONS

ω -terminated PMMA macromonomer was shown to copolymerize with *n*-BA monomer and the copolymerization reactivity ratio was estimated. The PMMA macromonomer exhibited reduced reactivity compared to MMA monomer in copolymerization with *n*-BA in bulk. The r_1 value for *n*-BA in *n*-BA/PMMA macromonomer copolymerization was determined to be 0.81. The reactivity of the PMMA macromonomer (r_2), was estimated by $1/r_1$ to be equal to 1.23. The values given in the literature for the *n*-BA/MMA system are; $r_1 = 0.43$ and $r_2 = 1.88$, or $r_1 = 0.11$ and $r_2 = 2.86$.²⁴ Using HPLC-silica adsorption chromatography, it was possible to separate the three types of species, i.e., PBA homopolymer, *n*-BA/PMMA macromonomer graft copolymer, and unreacted PMMA macromonomer, coexisting in the copolymer latex. The area under the macromonomer peak in the HPLC-silica adsorption spectra indicated a near-complete incorporation of the macromonomer into the PBA particles. From the DMS spectra, the degree of grafting increased with the ratio of PMMA macromonomer to *n*-BA. It was also observed that, with higher amounts of macromono-

mer (higher or equal to 10% weight of macromonomer based on total polymer phase), the grafted segments of PMMA macromonomer aggregated to form the PMMA domains in PBA matrix. These PMMA macromonomer domains work as a crosslinking site and a reinforcing filler in the soft PBA phase. When these seed latexes containing *in situ*-formed compatibilizing agent are used in the synthesis of PBA/PMMA composite latex particles, an improvement of mechanical properties can be expected from particles with a higher degree of PMMA macromonomer grafted. Data regarding the composite latexes will be presented in following papers.

We thank Dr. M. Fryd and Dr. B. L. Neff, E. I. duPont de Nemours and Company., Inc., for providing the PMMA macromonomer and the HPLC analysis; Dr. M. S. Vratsanos and Mr. S. Voth, Air Products and Chemicals, Inc., for the use of the RSA II; and Mr. W. Chotirotukon for his RSA data on the *n*-BA/20% PMMA macromonomer copolymer.

REFERENCES

1. D. R. Paul, *Polymer Blends*, Vol. 2, D. R. Paul and S. Newman, Eds., Academic Press, New York, 1978, p. 35.
2. J. P. Kennedy, *Recent Advances in Polymer Blends, Grafts, and Blocks*, L. H. Sperling, Ed., Plenum Press, New York, 1973, p. 3.

3. R. Milkovich and M. T. Chiang, U.S. Patents 3,786,116 (1974), 3,842,059 (1974), 3,862,101, 1975, to CPC International Inc.
4. R. Milkovich, *Anionic Polymerization Kinetics, Mechanisms, and Synthesis*, J. E. McGrath, Ed., ACS Symposium Series 166, American Chemical Society, Washington DC, 1981, p. 41.
5. Y. Kawakami, *Encyclopedia of Polymer Science and Technology*, Vol. 9, H. F. Mark, N. M. Bikales, C. G. Overberger, and G. Menges, Eds., Wiley-Interscience, New York, 1985, p. 195.
6. G. F. Meijs and E. Rizzardo, *J. Macromol. Sci., Rev. Macromol. Chem. Phys.*, **30**, 305 (1990).
7. G. O. Schulz and R. Milkovich, *J. Appl. Polym. Sci.*, **27**, 4773 (1982).
8. J. P. Kennedy and C. Y. Lo, *Polym. Bull.*, **13**, 441 (1985).
9. W. Chotirotukon, M.S. Thesis, Lehigh University, (1991).
10. Y. Tsukahara, M. Tanaka, and Y. Yamashita, *Polym. J.*, **19**, 1121 (1987).
11. V. Jaacks, *Makromol. Chem.*, **161**, 161 (1972).
12. P. Rajatapiti, V. L. Dimonie, and M. S. El-Aasser, *J. Macromol. Sci., Chem.*, **32**, 1445 (1995).
13. N. S. Enikolopyan, B. R. Smirnov, G. V. Ponomarev, and I. M. Belgovskii, *J. Polym. Sci., Polym. Chem. Ed.*, **19**, 879 (1981).
14. A. F. Burczyk, K. F. O'Driscoll, and G. L. Rempel, *J. Polym. Sci., Polym. Chem. Ed.*, **22**, 3255 (1984).
15. R. A. Sanayei and K. F. O'Driscoll, *J. Macromol. Sci., Chem.*, **26**, 1137 (1989).
16. G. O. Schulz and R. Milkovich, *J. Polym. Sci., Polym. Chem. Ed.*, **22**, 1633 (1984).
17. K. Ito, H. Tsuchida, A. Hayashi, T. Kitano, E. Yamada, and T. Matsumoto, *Polym. J.*, **17**, 827 (1985).
18. J. P. Kennedy and C. Y. Lo, *Polym. Bull.*, **13**, 343 (1985).
19. K. Muhlbach and V. Percec, *J. Polym. Sci., Polym. Chem. Ed.*, **25**, 2605 (1987).
20. Y. Gnanou and P. Lutz, *Makromol. Chem.*, **190**, 577 (1989).
21. P. Cacioli, D. G. Hawthorne, R. L. Laslett, E. Rizzardo, and D. H. Solomon, *J. Macromol. Sci., Chem.*, **23**, 839 (1986).
22. D. H. Solomon, *The Chemistry of Organic Film Formers*, Third Ed., Robert E. Krieger Publishing Co., Florida, 1982, p. 52.
23. D. S. Harrison, M.S. Thesis, Swinburne Institute of Technology, Australia, 1988.
24. *Polymer Handbook*, Third Ed., J. Brandrup and E. H. Immergut, Eds., Wiley-Interscience, New York, 1989, p. II-159.
25. *Polymer Handbook*, Third Ed., J. Brandrup and E. H. Immergut, Eds., Wiley-Interscience, New York, 1989, p. II-160.
26. T. H. Mourey, *J. Chromatogr.*, **357**, 101 (1986).
27. B. L. Neff and H. J. Spinelli, *J. Appl. Polym. Sci.*, **42**, 595 (1991).
28. L. H. Sperling, *Introduction to Physical Polymer Science*, Second Ed., John Wiley and Sons, New York, 1992, Ch. 8.
29. *Polymer Handbook*, Third Ed., J. Brandrup and E. H. Immergut, Eds., Wiley-Interscience, New York, 1989, p. VI-215.
30. *Polymer Handbook*, Third Ed., J. Brandrup and E. H. Immergut, Eds., Wiley-Interscience, New York, 1989, p. VI-219.

Received September 29, 1995

Accepted November 29, 1995